JOURNAL OF MECHANICS OF CONTINUA AND MATHEMATICAL SCIENCES
www.journalimcms.org

ISSN (Online) : 2454 -7190 Vol.-19, No.-6, June (2024) pp 99-127 ISSN (Print) 0973-8975

CYCLONE STABILITY PARAMETER: ITS NUMERICAL VALUE AND SIGNIFICANCE IN THE PERSPECTIVE OF TRACK DETERMINATION

Indrajit Ghosh[1], Sukhen Das[2], Nabajit Chakravarty[3]

[1]Dept. of Basic Sciences, College of Engineering and Management Kolaghat, East Medinipur, West Bengal, 721171 India

[1]Department of Atmospheric Sciences, University of Calcutta Kolkata, 700019, India.

[2]Dept. of Physics, Jadavpur University, Kolkata, West Bengal, 700032, India

[3] Positional Astronomy Centre, India Meteorological Department, Ministry of Earth Science, Salt Lake City, Kolkata, 700091, India.

[3] Department of Applied Optics & Photonics, University of Calcutta, Kolkata, West Bengal, 700106, India.

[3] Department of Atmospheric Sciences, University of Calcutta, Kolkata, 700019, India.

Email : [1]indraghosh06@gmail.com, [2]sukhendas29@gmail.com, [3]nabajit_c@yahoo.com

Corresponding Author: **Sukhen Das**

https://doi.org/10.26782/jmcms.2024.06.00008

(Received: April 13, 2024; Revised: May 21, 2024; Accepted: June 01, 2024)

Abstract

The study of the dynamics of tropical cyclones constitutes a major portion of the curriculum for atmospheric science throughout the world. This is due to its enormous significance on the coastal human civilization all over the world. The increase in sea surface temperature globally has led to an increase in the frequency of tropical cyclones. As many as ten deadly tropical cyclones have hit the Coromandel Coast of the Bay of Bengal Coastline after generating as depressions from the Bay of Bengal in the last decade. The most challenging part lies in the early detection of tropical depressions in the ocean bed, the consequent intensity prediction of the generated tropical cyclone and the forecasting of the resulting path of propagation of the cyclone in landmass. For these a detailed analytic study of the related cyclone dynamics governing equations, their corresponding solution, propounding of the cyclone analytic solution model and estimation of some critical *parameters based on real cyclone data for the validation of the analytic model is of utmost importance. Radio Sonde Radio Wind (RSRW) data analysis for 5 cyclones and subsequent Cyclone Stability Parameter (CSP)determination, simplification of the complicated expression of CSP and its subsequent significance is the main work of this paper. The CSP is the representative of the entire analysis of the governing equations of tropical cyclones in the applicable coordinate system of a previously performed important work. So this work is also a validation of the previously performed analytic work. We have also analytically simplified the expression of CSP through some approximations and chalked out a more lucid expression which is a function of r only. This work effectively unites analytic and numerical performances for more effective prediction of tropical cyclone path of propagation in landmass after their formation in tropical oceans.*

Keywords: Cyclone Stability Parameter (CSP), Cross Radial Velocity, Radio Sonde Radio Wind (RSRW), Track Determination, Transverse Velocity, Tropical Cyclone.

I. Introduction

A major scaled atmospheric whirlwind characterized by acute low-pressured core and vigorous outer layered wind motions is defined as a tropical cyclone. Nelson in 2014 described the Coriolis force dynamics from the earth's rotation in different hemispheres. The word 'tropical' in tropical cyclones relates to its development and genesis in tropical oceans. In the last decade, mainly in the tropical oceans the generation and strength of tropical cyclones have highly enhanced throughout the cyclone-prone coastal regions in the world. The tracks and intensities of tropical cyclones for the last 150 years are given by Liu (2010). A compact review of the important works performed on the topic of tropical cyclones so far can be obtained from Ghosh et al. (2021). The dynamical intensity variation of tropical cyclone Noru with numerical simulations was studied by Li and Xuyang (2020). Tropical cyclones completely devastate the coastal communities of the world in terms of threatening millions of lives and causing damage to properties and infrastructure worth billions of dollars. Global climate change has greatly affected the nature of climate-related natural hazards (Köhle et al. 2016). A significant portion of the global human population is prone to tropical cyclones since they stay in the proximity of the long global coastline. Rezapour (2015) described the impact of tropical cyclones and Tsunamis on them. The average life cycle of a tropical cyclone is 9 days and it includes four stages viz. formative, immature, mature, and decay stages respectively. The formative stage also known as the genesis stage is the first stage of the life span of tropical cyclones where it develops from an area of strong convective cloud. In this stage, there is no closed isobar at the surface. The second stage is an immature stage called the tropical depression stage where the tropical cyclone dynamics is most unstable. In this stage, the beginning of the gale force winds occurs and the official name of the cyclone is also given to the present strong depression. In tropical cyclone lifecycle, viz. when it enters landfall is known as the tropical storm stage. The fourth but last stage of the life cycle of a tropical cyclone is called the hurricane stage. This stage is called the decay stage and it includes the process for the cyclone to continue its progress over the cooler waters to land until it dissipates.

Emanuel (2005) defined a power dissipation index for describing the intensity of tropical cyclones. This index shows a marked increase in recent years due to the enhancement of the temperature of the surface of the sea. This is acts as a significant factor behind cyclone formation. In this context, the significance of anomaly temperature deserves special mention. Ghosh et al. (2022b) showed a special technique of anomaly temperature analysis that can help to forecast cyclone formation from developed depression in the ocean bed. Nott (2003) also studied similarly to determine the dynamics of cyclones that have struck in the past. Baisya et al. (2020) analyzed cyclone Phailin and Hudhud using the Weather Research and Forecasting (WRF) and The Coupled Ocean Atmosphere Wave Sediment Transport (COAWST) models. Tapiador (2008) recognized hurricanes using the Global Climate Model (GCM) of low resolution. In this work, we have analyzed the Radio Sonde and Radio Wind (RSRW) data of 5 tropical cyclones. Posada et al. (2012) performed a detailed analysis of RSRW data to verify the Fifth Generation/ NCAR Mesoscale Model (MM5) of the Madrid Barajas Airport. Tropical cyclones become more devastating in plane landforms leading to the sea compared to rugged landforms (Lala et al. 2014). The techniques adopted by IMD in the path forecasting of tropical cyclones generated in the Indian Ocean, Arabian Sea, and Bay of Bengal can be obtained from the work of Sikka (2006). The important works of Jung et al. (2010), Elsberry et al. (2010) and Spiridonov et al. (2020) in the field of cyclone path forecasting and thunderstorm alert also deserve mention. Storm surge resulting as a result of tropical cyclones is the most devastating factor affecting the damage of coastline areas. Siahsarani et al. (2020) showed the function of the Simulating Waves Nearshore Model (SWAN) for the Gulf of Oman.

II. Tropical Cyclone internal geometry

We can get an idea of tropical cyclone structure through a literature survey. Ritchi and Vigh (2010) did important work regarding tropical cyclone internal structural dynamics. Their work consisted of a summarized form of all important works done in the research of tropical cyclone internal structural dynamics that occurred between 2006 to 2010. Shevtsov et al. (2015) derived the relationship between tropical cyclone internal geometry and its devastation effect. Stern et al. (2015) derived a mutual relationship between intensification and contraction of cyclone eyewall. The total wind field consisting of fluxes (Ghosh and Chakravarty 2018) may be divided into three regions:-

II.i. The eye

The eye is the innermost part of a tropical cyclone. Here the atmosphere is most calm compared to the other portions of the cyclone. The radial extension of the eye from the axial line of the cyclone is from $30 - 65\mathrm{Km}$. The eye temperature is around $5.5^{0}\mathrm{C}$ warmer compared to the temperature of the other parts of the cyclone. As a result of this, light hot and sultry air containing a huge amount of moisture is abundant in the cyclone eye. A calm environment in the cyclone eye helps to condense the huge amount of moisture present in this region. Thus huge amount of potential energy is released and that acts as a fueling factor for the cyclone.

II.ii. The eyewall

The most destructive part of a tropical cyclone is the eyewall. The wind speed is strongest in eyewall and the rainfall is heaviest. Due to a very acute low pressure in the eye, the winds are driven by a very strong pressure gradient force in the eye wall. The circling horizontal or cross radial- winds can achieve a velocity of around $225 \mathrm{Km/hr}$.

II.iii. The wall cloud region

The region of strong wind perturbation extending from the eye wall to the spiral bands is called the wall cloud region. In this wall cloud region, the radial wind velocity extends considerably. This region extends up to a width of around 8 Km from cyclone axis.

II.iv. Rain bands

The rain bands prevail as bands encircling the center after the wall cloud region. They rotate apparently about the center. This portion is characterized by heavy rainfall with a decaying velocity of cross-radial wind.

The details anatomical picture of a tropical cyclone is given by Zhender (2019) in Fig.1

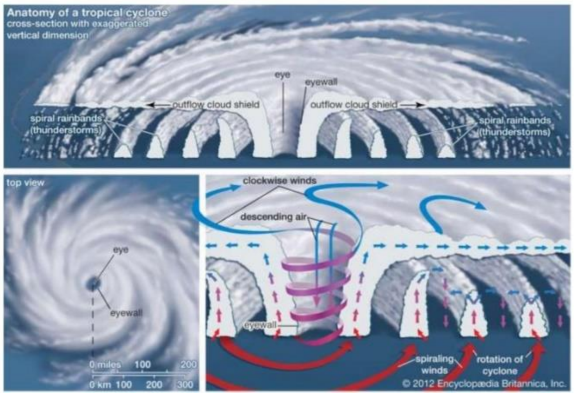

Fig. 1. Internal structural geometry of a tropical cyclone (Zehnder, 2018; "Anatomy of a Tropical Cyclone", courtesy of Encyclopædia Britannica, Inc., copyright 2018; used with permission)

III. Methodology and CSP analysis of cyclones

The Navier- Stoke's equation (Ghosh and Chakravarty 2018) in cylindrical coordinate system for a fluid parcel in a steady state is given by:-

$$u\frac{\partial v}{\partial r}+\frac{uv}{r}+w\frac{\partial v}{\partial z}+fu=\frac{\partial}{\partial r}\left[k_r\left(\frac{\partial v}{\partial r}+\frac{v}{r}\right)\right]+\frac{1}{\rho}\left[\frac{\partial}{\partial z}\left(\rho k_z\frac{\partial v}{\partial z}\right)\right] \tag{1}$$

The transport equation is given by:-

$$\frac{\partial}{\partial r}(\rho ur)+\frac{\partial}{\partial z}(\rho wr)=0 \tag{2}$$

The ideal gas equation is given by:-

$$p = \rho RT \tag{3}$$

The gravitational equilibrium equation is given by:-

$$\frac{\partial p}{\partial z} = -g\rho \tag{4}$$

From the works of Ghosh and Chakravarty (2018) tangential velocity necessary for attributing the whirlwind turbulence for a tropical cyclone in a cylindrical polar coordinate system having parameters (r, θ and z), is obtained from equations (1), (2), (3) and (4) and its given by,

$$V = \frac{1}{[f(r)]^{\frac{1}{4}}}\left\{\left(\frac{r}{r_1}\right)^{-\frac{Ar_1^2+1}{2k_r}}\right\}\exp\left\{\frac{A}{4k_r^2}(r^2-r_1^2)\right\}\Big(C_1\exp\left[-B^{\frac{1}{4}}\left\{r-\frac{\sqrt{B}}{10}r^5+\frac{G}{2\sqrt{B}r}-\frac{H}{4\sqrt{B}}r^2\right\}\right] + C_2\exp\left[\sqrt[4]{B}\left\{r-\frac{\sqrt{B}}{10}r^5+\frac{G}{2\sqrt{B}r}-\frac{H}{4\sqrt{B}}r^2\right\}\right]\Big) \tag{5}$$

Where the unknown constants are defined respectively as: k_r– Along the radial direction, the viscosity coefficient/unit mass for moist atmospheric air attributed to the cause of tropical cyclone.

k_z - The viscosity coefficient for moist atmosphere/ unit mass along the vertical direction.

$\rho$is the moist air density at vertical height z given by $\rho_0 e^{\left(\frac{-g}{RT}\right)}z$, where ρ_0 being the standard sea level density having a constant magnitude of $1.225\ \mathrm{kg/m^3}$

r_1 - The eye wall radius.

r_2 - The wall cloud radius.

$$P = \frac{1}{k_r}\left[\frac{1}{r}(Ar_1^2+1) - Ar\right]$$

$$Q = -\frac{1}{k_r}\left[\frac{1}{r^2} + A\left(1-\frac{r_1^2}{r_2^2}\right)\right]$$

$$R = fA\left(r - \frac{r_1^2}{r}\right)$$

$$A = -\frac{C\lambda k}{2}e^{-\frac{7H}{10}}.$$

$f, k, \lambda$are specific constants (Ghosh and Chakravarty 2018).

C_1andC_2 are also constants.

$$f(r) = Br^4 + \frac{G}{r^2} - Hr - \sqrt{B}$$

$$B = \frac{A^2}{4k_r^2},$$

$$G = \frac{3Ar_1^2}{2k_r} - \frac{1}{2k_r} + \frac{1}{4k_r^2} + \frac{Ar_1^2}{4k_r^2}, H = \frac{A}{2k_r}(Ar_1^2+1)$$

Here as $Z = 0; \frac{\partial V}{\partial Z} = 0; r = r_1$. The θ variation of V has also been considered negligible. The constants C_1 and C_2 are given by,

$$C_1 = 3000\exp\left[B^{1/4}\left\{r_1 - \frac{\sqrt{B}}{10}r_1^5 + \frac{G}{2\sqrt{B}r_1} - \frac{H}{4\sqrt{B}}r_1^2\right\}\right]$$

$$C_2 = 3000\exp\left[-B^{1/4}\left\{r_1 - \frac{\sqrt{B}}{10}r_1^5 + \frac{G}{2\sqrt{B}r_1} - \frac{H}{4\sqrt{B}}r_1^2\right\}\right]$$

The solution of the corresponding radial velocity of the considered fluid parcel taken as a representative of the cyclone fluid parcel is given by,

$$U = \alpha(r^2 - r_1^2)e^{\left(z-\frac{7H}{10}\right)} \tag{6}$$

Where $Z \leq H$,

Also

$$U = \alpha(r^2 - r_1^2)e^{-\left(z-\frac{7H}{10}\right)} \tag{7}$$

Where $Z > H$

Here the constant α is given by, $\alpha = 0.000292$ SI unit and $H = 20$Km is the upper troposphere height of the tropical cyclone.

III.i. *CSP* simplification and its significance

In our work (Ghosh and Chakravarty 2018) we have shown that $CSP = \frac{V}{U}$ is a crucial parameter for determining the stability of a cyclone.

Where V and U are respectively the radial and cross-radial velocity of a concerned fluid parcel within the cyclonic system at a certain instant of time. If we expand the exponential terms of equation (5) and use the approximation $\exp(x) = 1 + x$ (when $x << 1$) then after some cancellation of terms the ultimate value of the cross radial velocity is given by,

$$V = \frac{6000}{\sqrt{f(r)}}\left[1 - \sqrt[2]{B}\left(r - \frac{\sqrt{B}}{10}r^5 + \frac{G}{2\sqrt{B}r} - \frac{Hr^2}{4\sqrt{B}}\right)^2\right] \tag{8}$$

Where $f(r) = Br^4 + \frac{G}{r^2} - Hr - \sqrt{B}$

Thus utilizing the expressions of U and V from equations (6),(7) and (8) we get the simplified expression of CSP as

$$CSP = \frac{12000r}{\alpha\sqrt[4]{f(r)}(r^2 - r_1^2)} \tag{9}$$

From the value of CSP we can readily conclude whether a low pressure system tends to form a cyclone in practice. If the numerical value of CSP exceeds unity then the concerned fluid parcel within the cyclone has a higher value of instantaneous cross radial velocity component than the corresponding instantaneous radial velocity component. As a result, we conclude the cyclone to be stable as the wind converges towards a point. The more the value of CSP the more stable the cyclonic system. So the numerical value of CSP is proportional to the stability aspect of a tropical cyclone and its critical value being unity. Reynolds number differentiates analogically laminar and turbulent flow in fluid dynamics. Thus the significance of CSP in cyclonic stability is analogous to the significance of Reynolds number in demarcating stable depression liable to form as a cyclone and non-stable depression liable to be dissipated. An account of CSP analysis from cyclone RSRW data can be obtained from the work of Ghosh et al. (2022a).

Our studies are as follows,

III.ii. Analysis of Cyclone Laila

Cyclone Laila first developed over the Bay of Bengal on 18th May 2010. It got strengthened as it moved north-westward and increased its strength on the next day. It made landfall near Bapatla of Andhra Pradesh on 20th May 2010 and dissipated on 21st May 2010. From the tables 1 to 4 along with the graphs 2 to 5, we try to predict the movement of the cyclonic system. As the *CSP* value is greater than unity the cyclonic system tends to get deflected towards Chennai.

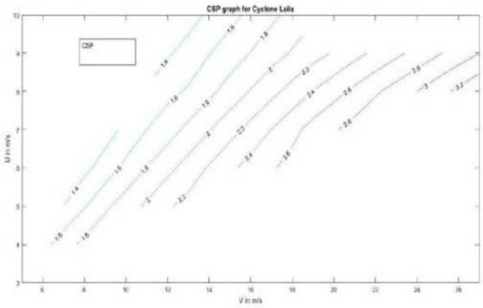

Fig. 2 *CSP* graph for cyclone Laila on 18th May 2010

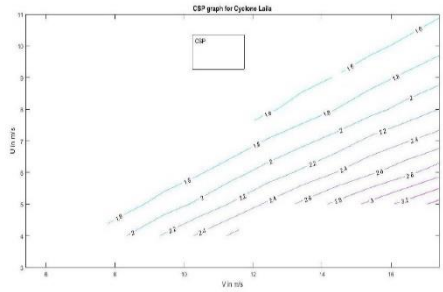

Fig. 3 *CSP* graph for cyclone Laila 18th on 19 May 2010

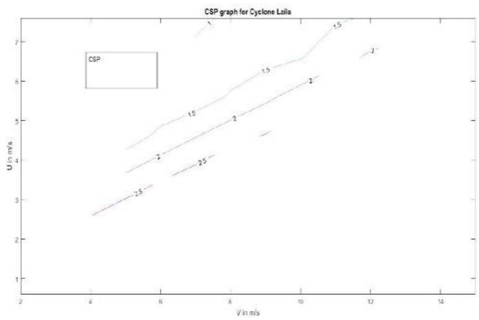

Fig. 4 *CSP* graph for cyclone Laila on 20th May, 2010

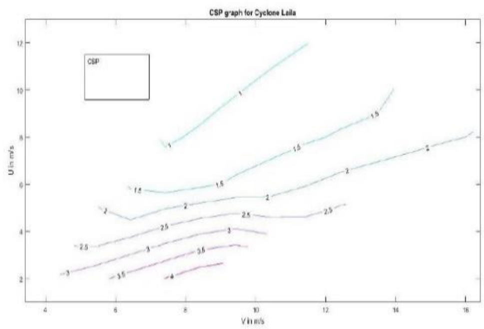

Fig. 5 *CSP* graph for cyclone Laila on 21th May, 2010

Table 1: Laila CSP on 18$^{\text{th}}$ May, 2010

Altitude (m)	Bhubaneswar wind velocity (U) in m/s	Chennai wind velocity (V) in m/s	CSP=V/U
70	3.000000000	5	1.666666667
150	3.883002207	6	1.545196134
300	5.207505519	7	1.344213650
448	6.514348786	11	1.688580142
600	8.000000000	13	1.625000000
681	8.000000000	14	1.750000000
920	8.652694610	18	2.080276817
1015	9.000000000	20	2.222222222
1416	8.537190083	26	3.045498548
1500	8.000000000	27	3.375000000
1932	9.000000000	27	3.000000000
2477	7.775747508	23	2.957914976
3100	7.255319148	20	2.756598241
4500	10.65067651	13	1.220579743

Table 2: Laila CSP on 19$^{\text{th}}$ May, 2010

Altitude (m)	Chennai wind velocity (V) in m/s	Bhubaneswar wind velocity (U) in m/s	CSP=V/U
45	2	0.600000000	3.333333
495	5	4.764705882	1.049383
552	6	5.266094420	1.139364
728	8	6.776824034	1.180494
943	10	8.000000000	1.250000
967	10	8.000000000	1.250000
1086	11	8.000000000	1.375000
1317	10	8.000000000	1.375000
1464	10	8.000000000	1.250000

1987	11	8.000000000	1.250000
2274	12	8.000000000	1.375000
2542	14	8.000000000	1.500000
2782	15	8.000000000	1.750000
3127	12	8.000000000	1.875000
3746	11	8.000000000	1.500000
4403	7	8.000000000	1.375000
5106	8	9.14	0.875000

Table 3: Laila CSP on 20^{th} May, 2010 (date of landfall)

Altitude (m)	Chennai wind velocity (V) in m/s	Bhubaneswar wind velocity (U) in m/s	CSP = V/U
45	5.404255319	6	1.801418440
321	17.12068966	7	2.853448276
478	18.00000000	9	2.571428571
712	18.00000000	10	1.8000000000
860	18.00000000	10	1.800000000
951	18.00000000	11	1.636363636
994	18.00000000	10	1.710927835
1447	17.10927835	11	1.448701299
1969	15.93571429	10	1.591785714
2254	15.91785714	8	1.880145798
2523	15.04116638	8	1.896012007
2560	15.16809605	6	2.672670097
2813	16.03602058	5	3.671936759
3438	18.35968379	7	2.557491289
3726	17.90243902	6	2.675813008
4029	16.05487805	6	2.262437812
4385	13.57462687	6	1.563153310
4932	12.50522648	8	1.659940209

5261	13.27952167	8	1.980568012
5652	13.86397608	7	2.336419753

Table 4: Laila CSP on 21st May, 2010

Altitude in m	Bhubaneswar Wind Velocity (U) in m/s	Chennai Wind Velocity (V) in m/s	CSP=V/U
45	1	3.418604651	3.41860465
493	2	9.115702479	4.55785124
726	4	11.05434783	2.76358696
809	4	11.50543478	2.87635870
965	5	12.00000000	2.4000000
1143	5	11.42212190	2.28442438
1396	6	10.27990971	1.71331829
1459	6	10.00000000	1.66666667
1978	6	7.043298969	1.17388316
2234	8	7.853503184	0.98168790
2378	8	9.301075269	1.16263441
2527	8	10.90322581	1.36290323
2689	8	11.78730703	1.47341338
2824	9	13.96397942	1.55155327
3107	8	16.87650086	2.10956261
3504	8	14.59875260	1.82484408
3724	9	13.08823529	1.45424837
4380	9	7.145454545	0.79393939
5081	10	7.936666667	0.79366667
5839	13	11.00000000	0.84615385

III.iii. Cyclone Phailin analysis

Cyclone Phailin developed as a severe cyclone on October 9, 2013, after passing into the Andaman Sea from the Malay Peninsula. It intensified further and developed as a severe cyclonic storm on 9th Oct 2013 and completely dissipated on 14th Oct 2013. By analyzing the RSRW data of Waltair and Bhubaneswar we calculated the CSP for Phailin for each day from 9th to 13th Oct, 2013 concerning the geopotential height within the boundary layer. We take the RSRW wind velocity of Bhubaneswar as the tangential velocity and the RSRW wind velocity of Waltair as the radial velocity of the cyclone wind respectively (Tables 5,6,7,8 and 9 which are self-explanatory). Here also graphs of U, V, and CSP (Figs. 6 to 10) are plotted and from the tables and subsequent graphs, we try to predict the movement of the cyclonic system. We observe that the cyclonic system tends to drift towards Bhubaneswar as the CSP value is greater than unity.

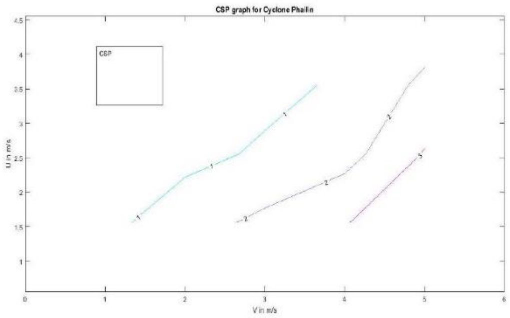

Fig.6. CSP graph for cyclone Phailin on 9^{th} Oct, 2013

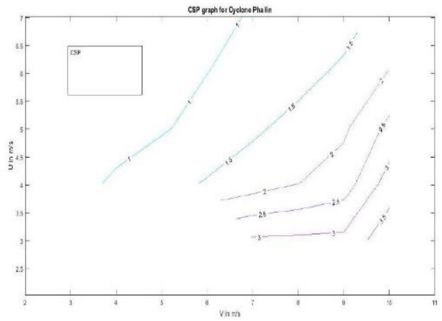

Fig. 7. *CSP* graph for cyclone Phailin on 10^{th} Oct, 2013

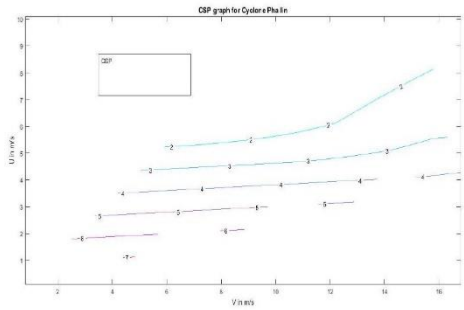

Fig. 8. *CSP* graph for cyclone Phailin on 11^{th} Oct

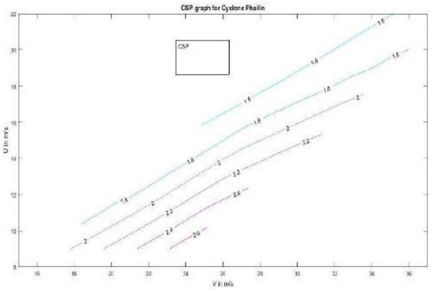

Fig. 9. *CSP* graph for cyclone Phailin on 12^{th} Oct, 2013

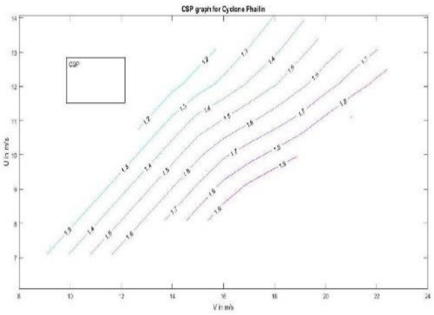

Fig.10. CSP graph for cyclone Phailin on 13^{th} Oct, 2013

Table 5: Phailin CSP on 9th Oct, 2013

Altitude (m)	Waltair wind velocity (U) in m/s	Bhubaneswar wind velocity (V) in m/s	CSP=V/U
51	1.939189189	1	0.515679443
72	1.000000000	1	1.000000000
521	0.939393939	5	5.322580647
993	0.556621880	6	10.77931036
1487	1.050909090	6	5.709342565
2007	2.045296167	4	1.955706985
2555	2.960975610	4	1.350906095
3133	1.096728307	3	2.735408561
4397	4.980263158	5	1.003963012
5098	3.970909092	4	1.007326007

Table 6 : Phailin CSP on 10th Oct, 2013

Altitude in m	Waltair wind velocity (U) in m/s	Bhubaneswar wind velocity (V) in m/s	CSP=V/U
56	4.094218415	2	0.488493724
75	4.256959314	3	0.704728370
530	8.000000000	7	0.875000000
764	8.000000000	6	0.750000000
1003	7.965794769	8	1.004294014
1497	7.000000000	10	1.428571429
2017	6.975155280	9	1.290293856
2564	6.004436557	8	1.332348160
3143	3.126623377	9	2.878504673
3757	6.000000000	8	1.333333333
4413	4.038235294	9	2.228696286
5115	2.023622047	11	5.435797666
5871	3.996372430	8	2.001815431

Table 7: Phailin CSP on 11th Oct, 2013

Altitude in m	Waltair wind velocity (U) in m/s	Bhubaneswar wind velocity (V) in m/s	CSP=V/U
6	0.1	0.800000000	8.000000000
84	6.0	6.194895591	1.032482599
538	8.0	8.050847458	1.006355932
772	7.0	11.75933610	1.679905157
1011	6.0	14.35685484	2.392809140
1506	4.0	17.00000000	4.250000000
2025	5.0	16.84840426	3.369680852
2570	6.0	15.39893617	2.566489362
3148	8.0	13.60864041	1.701080051
3764	11	12.23708207	1.112462006
4419	11	15.03393352	1.366721229
5119	10	15.51869806	1.551869806
5874	9.0	16.00000000	1.777777778

Table 8: Phailin CSP on 12th Oct, 2013 (date of landfall)

Altitude (m)	Bhubaneswar wind velocity (V) in m/s	Waltair wind velocity (U) in m/s	CSP=V/U
48	15	8.000000000	1.875000000
480	24	8.717557251	2.753064799
712	21	12.36170213	1.698795181
949	28	17.11445783	1.636043647
1442	33	20.08076923	1.643363340
1961	36	22.97542533	1.566891558
2509	36	21.89170897	1.644458185
3089	37	19.96563011	1.853184688
3706	34	19.08256881	1.781730769

4362	30	21.04113475	1.425778617
5066	32	22.00000000	1.454545455

Table 9: Phailin CSP on 13th Oct, 2013

Altitude (m)	Bhubaneswar wind velocity (V) in m/s	Waltair wind velocity (U) in m/s	*CSP*=V/U
49	8	6.081632653	1.315436242
498	17	13.76171875	1.235310815
732	18	13.16455696	1.367307692
972	16	12.00000000	1.333333333
1468	14	12.24712644	1.143125293
1989	17	14.76880734	1.151074668
2536	17	11.92478632	1.425602065
3117	19	10.80707395	1.758107707
3736	17	8.223564954	2.067229978
4397	18	12.00000000	1.500000000
5103	21	12.04188482	1.743913043
5866	24	12.88768116	1.862243464
6696	19	10.00000000	1.900000000

III.iv. Cyclone Helen analysis

Severe cyclonic storm Helen struck the Coromandel Coast (near Machlipatnam, Andhra Pradesh) on 21st Nov 2013 just one month after the striking of tropical cyclone Phailin. It developed as a weak depression over the Bay of Bengal from the remains of tropical storm Podul. It then started gaining momentum on the following two days of the 19th and 20th Nov traveling northwest and ultimately made landfall on 21st Nov, over Machlipatnam as a severe cyclonic storm. The cyclone dissipated on 22nd Nov, 2013. Analyzing the RSRW data of Waltair and Bhubaneswar we calculated the concerned CSP for Helen from 18th to 23rd Nov respectively with corresponding geopotential heights within the boundary layer taking the Waltair wind velocity as the tangential cyclone wind velocity and the Bhubaneswar wind velocity as the radial cyclone wind velocity respectively (Tables 10 to 15, which are self-explanatory). Then we plot the figures of $U, V,$ and CSP (Figs. 11 to 16) and hence we try to estimate the movement track of the cyclone. It's observed from the graphs and tables that the cyclonic system tends to drift towards Waltair as CSP is greater than unity.

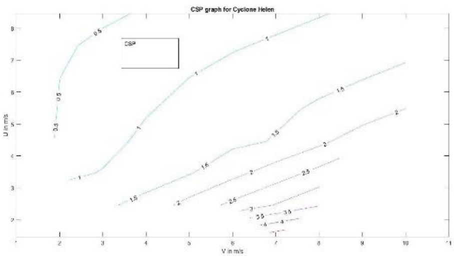

Fig.11. CSP graph for cyclone Helen on 18^{th} Nov, Nov, 2013

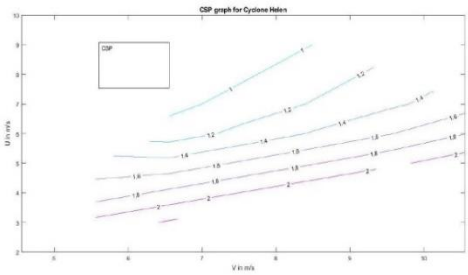

Fig. 12. Cyclone Helen CSP graph on 19^{th} Nov, 2013

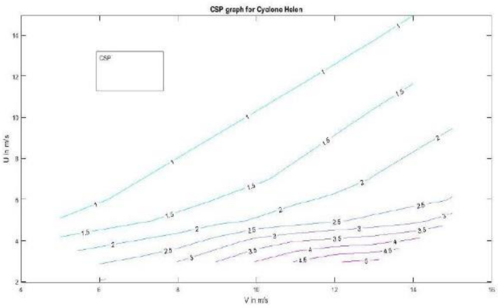

Fig. 13. Cyclone Helen *CSP* graph on 20^{th} Nov 2013

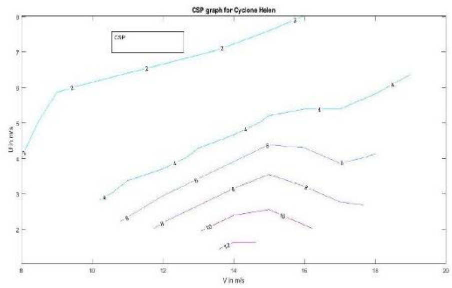

Fig. 14. Cyclone Helen CSP graph on 21^{st} Nov 2013

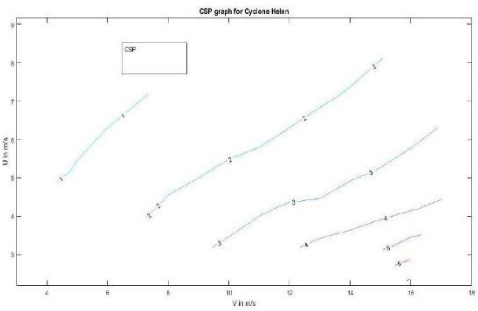

Fig. 15. Cyclone Helen *CSP* graph on 22^{nd} Nov 2013

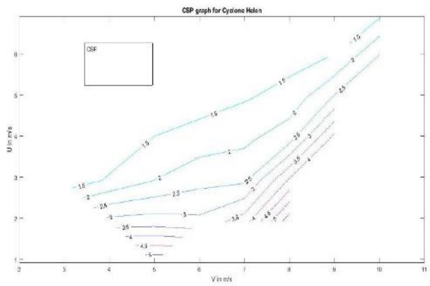

Fig. 16. Cyclone Helen CSP graph on 23^{rd} Nov 2013

Table 10: Helen CSP on 18th Nov 2013

Altitude (m)	Waltair wind velocity (V) in m/s	Bhubaneswar wind velocity (U) in m/s	CSP=V/U
45	3.0	1.875000000	1.600000
80	4.0	3.263157895	1.225806
531	10	8.650224215	1.156039
763	11	6.482608696	1.696848
1001	9.0	5.148000000	1.748252
1495	8.0	2.189000000	3.654637
2015	6.0	2.054158670	2.920903
2563	7.0	1.458715590	4.798742
3143	6.0	1.920415225	3.124324
3757	4.0	2.000000000	2.000000
4411	4.0	2.976851851	1.343701
5113	4.0	2.011510791	1.988555
5867	1.0	8.962666667	0.111574
6686	1.0	5.000000000	0.200000

Table 11: Helen CSP on on 19th Nov 2013

Altitude (m)	Waltair wind velocity (V) in m/s	Bhubaneswar wind velocity (U) in m/s	CSP=V/U
41	4.555000000	2.0	2.277500000
113	6.334075724	7.0	0.904867961
558	10.88793103	7.0	1.555418719
789	9.894514768	6.0	1.649085795
1026	10.74645030	5.0	2.149290060
1518	6.046242775	6.0	1.007707129
2034	7.000000000	7.0	1.00000000
2589	6.896551724	10	0.689655172
2692	7.458620689	10	0.745862069

Table 12 : Helen CSP on 20^{th} Nov, 2013

Altitude (m)	Bhubaneswar wind velocity (U) in m/s	Waltair wind velocity (V) in m/s	CSP=V/U
45	2.287581699	7.0	3.066666667
69	7.895386134	16	2.062500001
519	5.16706855	15	2.903030303
751	15.65294925	14	0.894400140
989	2.069246436	13	6.282480314
1480	4.819066148	13	2.697618086
1997	5.948339483	13	2.185483871
2542	5.045217391	9.0	1.783867632
3119	6.930807249	10	1.442833373
3731	2.018575851	6.0	2.972392639
4386	2.000000000	7.0	3.500000000
5087	5.000000000	4.0	0.800000000

Table 13: Helen CSP on 21^{st} Nov, 2013 (date of landfall)

Altitude (m)	Waltair wind velocity (V) in m/s	Bhubaneswar wind velocity (U) in m/s	CSP = V/U
45	10	2.063829787	4.845360825
483	20	8.256558040	2.422316891
735	17	8.130434783	2.090909091
963	15	7.311926606	2.051442911
1457	18	7.042876902	2.555773763
1969	16	8.875243665	1.802767406
2512	16	6.161111111	2.596934175
3090	18	2.160839161	8.330097087
3705	14	1.027914614	13.61980831
4361	10	3.000000000	3.333333333
5064	8.0	3.992826399	2.003593245
5819	8.0	8.000000000	1.000000000

Table 14: Helen CSP on 22^{nd} Nov 2013

Altitude (m)	Bhubaneswar wind velocity (U) in m/s	Waitair wind velocity (V) in m/s	CSP = V/U
45	2.872340426	8.0	2.785185185
491	3.470852018	13	3.745478036
733	9.207792208	15	1.629055007
961	7.481012658	13	1.737732657
1455	7.000000000	12	1.714285714
1970	4.303501946	13	3.020795660
2515	2.184162063	16	7.325463742
3090	2.916230366	15	5.143626572
3702	4.801916933	18	3.748502994
4357	5.942766295	8.0	1.346174425
5062	6.961206896	5.0	0.718266254
5821	6.027888446	9.0	1.493060145
6646	3.941176471	6.0	1.522388060
7550	5.033407572	3.0	0.596017699

Table 15 : Helen CSP on 23^{rd} Nov, 2013

Altitude (m)	Bhubaneswar wind velocity (U) in m/s	Waltair wind velocity (V) in m/s	CSP = V/U
45	0.918367346	5.0	5.444444450
75	1.800000000	6.0	3.333333333
524	7.575892857	11	1.451974072
757	5.478448276	9.0	1.642800944
995	4.151898734	8.0	1.926829268
1488	2.142276423	6.0	2.800759013
2005	2.000000000	7.0	3.500000000
2551	2.941176470	7.0	2.380000000
3128	1.101045296	8.0	7.265822786

3742	1.921182266	6.0	3.123076923
4395	5.797235023	8.0	1.379968204
5096	5.103305785	5.0	0.979757085
5853	3.015978695	2.0	0.663134658

III.v. Cyclone Hudhud analysis

Cyclone Hudhud developed as a very severe cyclonic storm on 11^{th} Oct, 2014 progressing towards the Bay of Bengal coast of Andhra Pradesh. It made landfall on 12^{th} Oct 2014 over Vishakapattanam and dissipated on 13^{th} Oct, 2014. Similarly as before we calculated the CSP for Hudhud with the geopotential by the analysis of RSRW data of Port Blair and Bhubaneswar. The corresponding analysis is given in self-explanatory tables 16 to 18. U, V and CSP are plotted in subsequent graphs (Figs. 17 to 19) and hence we try to predict the movement of this cyclone system. Here also by observing the tables and graphs, we see that the cyclonic system tends to drift towards Bhubaneswar as the CSP value is greater than unity.

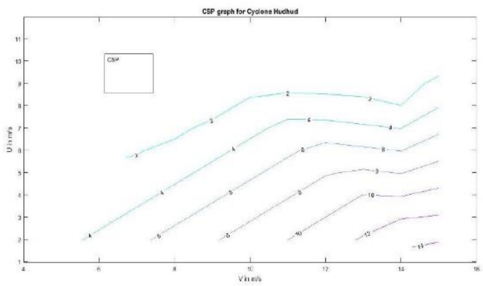

Fig. 17. Cyclone HudhudCSP graph on 11^{th} Oct, 2014

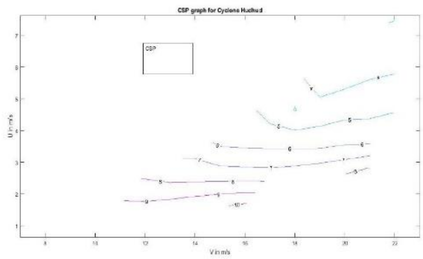

Fig. 18. Cyclone HudhudCSP graph on 12^{th} Oct 2014

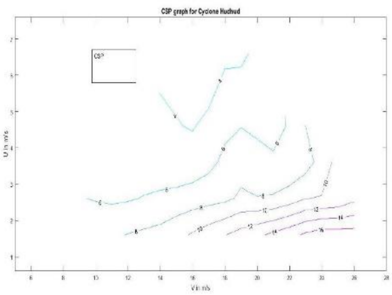

Fig. 19. Cyclone HudhudCSP graph on 13^{th} Oct 2014

Table 16: CSP analysis for cyclone Hudhud on 11th Oct 2014

Altitude (m)	Port Blair wind velocity (U) in m/s	Bhubaneswar wind velocity (V) in m/s	VSP /U
56	1.358200000	4.0	2.945074363
485	12.78297872	9.0	0.704061252
958	10.43514644	14	1.341619888
1454	10.28352490	13	1.264157973
1975	10.61621967	16	1.507127820
2525	0.967432960	15	15.50495034
3107	9.165803109	14	1.527416620
3725	9.960948396	15	1.505880706
4387	8.114365411	14	1.725335167
5096	9.206865402	10	1.086145997

Table 17: CSP analysis for cyclone Hudhud on 12th Oct, 2014 (date of landfall)

Altitude (m)	Port Blair wind velocity (U) in m/s	Bhubaneswar wind velocity (V) in m/s	CSP = V/U
67	0.634469697	7.0	11.03283582
500	4.734848485	18	3.801600000
973	7.287465940	21	2.881660123
1468	7.961852861	22	2.763175907
1988	7.057471264	21	2.975570033
2536	5.627208481	23	4.087284144
3114	4.095406360	22	5.371872304
3730	3.115853659	20	6.418786692
4388	2.112805000	21	9.939393366
5092	5.778110945	19	3.288271925

Table 18: CSP analysis for cyclone Hudhud on 13$^{\text{th}}$ Oct 2014

Altitude (m)	Port Blair wind velocity (U) in m/s	Bhubaneswar wind velocity (V) in m/s	CSP = V/U
53	0.654320987	5.0	7.641509442
49	0.604938271	5.0	8.265306131
506	3.876379691	16	4.127562642
739	8.000000000	18	2.250000000
977	8.000000000	18	2.250000000
1987	2.127413127	19	8.931034484
3109	3.931153184	22	5.596322242
3722	1.204878049	24	19.91902834
4376	1.935779816	28	14.46445498
5839	2.942257217	23	7.817127567

III.vi. Cyclone Vardah analysis

Cyclone Vardah was also a highly intense storm that struck Andaman and Nicobar Islands and some portion of southern India on 12$^{\text{th}}$ December, 2016. We analyzed the RSRW data of Bhubaneswar and Waltair to calculate its CSP with geopotential height within the boundary layer taking the RSRW wind velocity over Bhubaneswar as the tangential cyclone wind velocity and the RSRW wind velocity over Waltair as the radial cyclone wind velocity respectively on 8$^{\text{th}}$ Dec 2016 (since the depression was nearer to Bhubaneswar than Waltair on that day). In the coming days till the day of dissipation $\left(9^{\text{th}}\right.$ to 13$^{\text{th}}$ December, 2016) we have analyzed as before in tables 19 to 24, which are again self-explanatory. We have again plotted the subsequent U, V, and CSP graphs (Figs. 20 to 25) and again tried to predict the movement of the cyclone system from these. Here also by observing the tables and graphs, we see that the cyclonic system tends to drift towards Waltair as the CSP value is greater than unity.

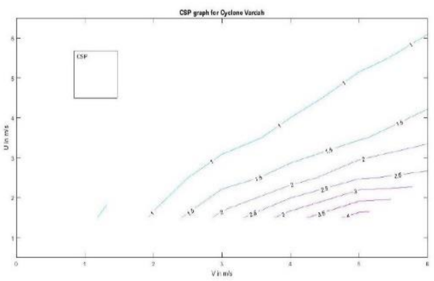

Fig. 20. Cyclone VardahCSP graph on 8$^{\text{th}}$ Dec, 2016

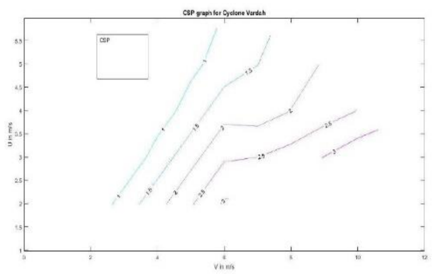

Fig. 21. Cyclone VardahCSP graph on 9$^{\text{th}}$ Dec, 2016

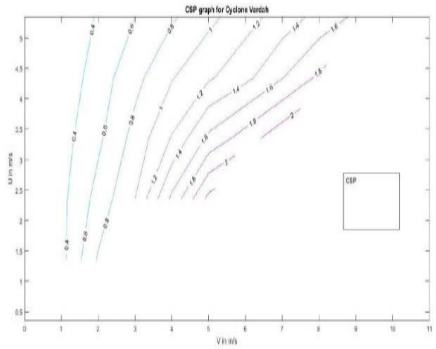

Fig. 22. Cyclone Vardah*CSP* graph on 10th Dec, 2016

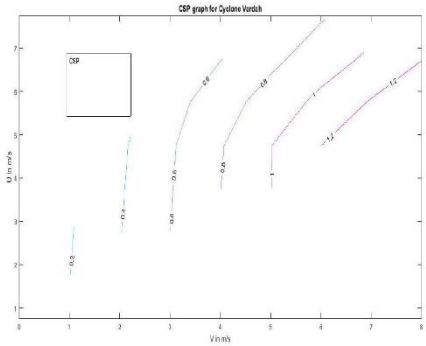

Fig. 23. Cyclone Vardah*CSP* graph on 11th Dec, 2016

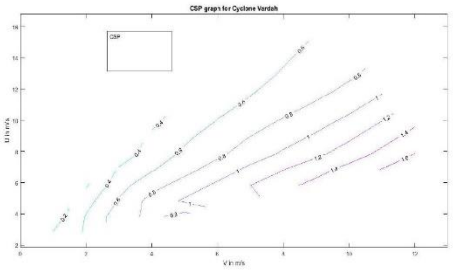

Fig. 24. Cyclone Vardah*CSP* graph on 12th Dec, 2016

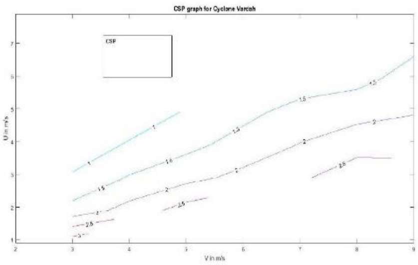

Fig. 25. Cyclone Vardah*CSP* graph on 13th Dec, 2016

Table 19: CSP analysis for Cyclone Vardah on 8th Dec 2016

Altitude (m)	**Bhubaneswar wind velocity (V) in m/s**	**Waltair wind velocity (U) in m/s**	***CSP*=V/U**
45	0.5	0.5	0
466	4.646799117	3.0	1.548933039
702	2.128205128	3.0	0.709401709
943	2.882845188	2.0	1.441422594
1441	5.000000000	4.0	1.25000000
1964	5.953934740	7.0	0.850562106
2515	6.000000000	6.0	1.000000000
3097	6.000000000	5.0	1.200000000
3714	6.000000000	2.0	3.000000000

4375	5.483996877	1.0	5.483996877
5084	5.967422096	4.0	1.491855524
5846	6.968545216	5.0	1.393709043

Table 20: CSP analysis for Cyclone Vardah on 9th Dec, 2016

Altitude (m)	Waltair wind velocity (V) in m/s	Bhubaneswar wind velocity (U) in m/s	CSP=V/U
45	0.978260869	0.86322966	1.133256785
467	6.0	1.935555555	3.099885190
703	8.0	2.884615384	2.773333334
945	10	3.000000000	3.333333333
1445	12	3.957575757	3.032159265
1966	10	4.000000000	2.500000000
2515	11	3.034608379	3.624849940
3097	9.0	3.967353851	2.27272723
3715	6.0	4.000000000	1.50000000
4377	6.0	5.975720789	1.0041841
5086	6.0	6.955497382	0.862627023

Table 21: CSP analysis for cyclone Vardah on 10th Dec, 2016

Altitude (m)	Waltair wind velocity (V) in m/s	Bhubaneswar wind velocity (U) in m/s	CSP = V/U
45	0	0.350000000	0
455	1.0	5.679814385	0.176062092
701	1.0	2.846808511	0.351270553
933	4.0	3.000000000	1.333333333
1432	4.0	3.963782696	1.009137056
1956	4.0	4.000000000	1.000000000
2507	8.0	4.000000000	2.000000000
3091	8.0	4.000000000	2.000000000
3710	5.0	2.038834951	2.452380953

4372	7.0	3.969696970	1.763358778
5081	5.0	4.000000000	1.250000000
5844	7.0	4.000000000	1.750000000
6679	11	5.996688742	1.834345665

Table 22: CSP analysis for cyclone Vardah on 11th Dec 2016

Altitude (m)	Waltair wind velocity (V) in m/s	Bhubaneswar Velocity (U) in m/s	CSP = V/U
45	0	0.750000000	0
464	2	5.686363636	0.351718625
700	4	6.906383979	0.579174285
942	4	6.083333334	0.657534247
1440	8	5.038229377	1.587859425
1963	6	7.965517241	0.753246753
2514	6	5.097272723	1.177100055
3096	8	7.912371134	0.758306189
3714	6	7.022764228	1.139152582
4374	8	6.015243902	0.997465788
5081	6	6.000000000	1.333333333
5844	6	5.013106160	1.196862745
6678	5.000000000	1.200000000	4.16666666

Table 23: CSP analysis for cyclone Vardah on 12th Dec 2016 (date of landfall)

Altitude (m)	Bhubaneswar wind velocity	Waltair wind velocity (V) in m/s	CSP= V/U
45	1.836734694	0	0
483	6.706401766	3.0	0.447333772
719	9.919491525	5.0	0.504058095
961	10.00000000	6.0	0.600000000
1459	12.90342052	11	0.852487136

1982	8.115606936	9.0	1.108974359
2531	7.016483516	13	1.852779953
3110	4.036395147	4.0	0.990983255
3724	7.973813421	7.0	0.877873563
4384	12.00711238	5.0	0.416419855
5091	16.97368421	8.0	0.471317829
5853	6.008403361	8.0	1.331468532

Table 24: CSP analysis for cyclone Vardah on 13th Dec 2016

Altitude (m)	Bhubaneswar wind velocity (U) in m/s	Waltair wind velocity (V) in m/s	CSP= V/U
45	1.836734694	0	0
483	6.706401766	3.0	0.447333772
719	9.919491525	5.0	0.504058095
961	10.00000000	6.0	0.600000000
1459	12.90342052	11	0.852487136
1982	8.115606936	9.0	1.108974359
2531	7.016483516	13	1.852779953
3110	4.036395147	4.0	0.990983255
3724	7.973813421	7.0	0.877873563
4384	12.00711238	5.0	0.416419855
5091	16.97368421	8.0	0.471317829
5853	6.008403361	8.0	1.331468532

IV. Result and Discussions

First of all, in this study we have analytically simplified the expression for CSP as obtained in Ghosh and Chakravarty (2018) by resolving the exponential terms present in the analytic solution of the cross radial velocity (Eqn. 5). Hence we obtained a simplified expression of CSP (Eqn. 9) which is a radial function only. When this expression of CSP is plotted w.r.t. r (shown in Fig. 26) we find that with the increase in the value of r, the value of CSP diminishes showing that the stability of cyclone is maximum at the cyclone core and minimum at the cyclone periphery. The simplified expression of V as obtained in Eqn. 8 from Eqn. 5 has helped to obtain the lucid expression of CSP (which is a function of r only) from the simplified expression of V (Eqn. 8) given in Eqn. 9. Also in this study we have used the velocity data which were obtained from RSRW observations of different India Meteorological Department (IMD) observatories. For the study, we have chosen 5 cyclones, viz. Laila, Phailin, Helen, Hudhud and Vardah. A CSP value greater than unity implies low pressure at coastal stations. The CSP analysis of prefix and suffix days of cyclone landfall of the five cyclones was done based on the availability of corresponding RSRW data.

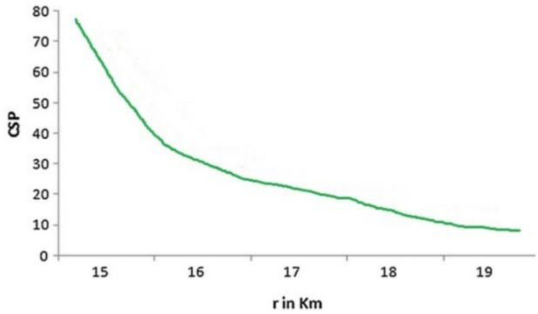

Fig. 26 Variation of CSP w.r.t. r

V. Conclusions

This work provides an excellent effective technique for determining the movement track of a tropical cyclone derived from the complicated theory of its dynamical equations. This work validates the theoretical solutions of Ghosh and Chakravarty (2018) by the CSP analysis of the observational data of five tropical cyclones of the Bay of Bengal basin. During the generation of a depression that tends to develop as a tropical cyclone, we take two representative places within the low-pressure belt viable to be affected by the cyclone, we then analyze the RSRW data of the wind velocity of those places within the boundary layer and calculate CSP for the cyclone taking the RSRW wind velocity of one place as the radial velocity component of the cyclone and the corresponding other place RSRW wind velocity as the cross-radial velocity component of the cyclone with the geopotential height. It is worthwhile to mention that the location of the chosen places for this analysis should be nearly normal to the path of propagation of the cyclone. Now if the CSP value increases and remains above unity then the cyclone will be stable and it will progress to a place close to the region for which we have taken the RSRW wind velocity as V (the cyclone cross radial or tangential velocity) for landfall. If the CSP value decreases and becomes less than unity then the cyclone is progressing to a place close to the region for which we have taken the RSRW wind velocity as U (cyclone radial velocity) for landfall. In fact in this work for all five cyclones from the corresponding tables and figures, we see that the cyclonic system tends to drift towards the place where the RSRW wind velocity is taken as the cross radial velocity of the cyclone as the CSP value is greater than unity. This is the most important conclusion and outcome from the detailed analysis carried out in this work. Apart from these an important simplification of the CSP expression has also been incorporated in this work. In future work, we can try to find out a critical parameter with the help of scale analysis, so that one can decide which depressions can become cyclones.

VI. List of Important Symbols

$A, B, C, C_1, C_2, G, H, P, Q$ and R-constants in equation (5) with applicable SI units.
CSP - Cyclone Stability Parameter (dimensionless quantity)
V - Cross radial velocity $(\mathrm{m/s})$
U-Radial Velocity (m/s)

VII. Acknowledgments

The authors are highly grateful to their present employers for allowing them to do this research and make it a success. They are also thankful to National Data Center (IMD Pune) for providing the necessary data for doing this research.

Conflict of Interest:

There was no relevant conflict of interest regarding this paper.

References

I. Baisya H., Pattanaik S., Chakraborty T., : 'A coupled modeling approach to understand ocean coupling and energetics of tropical cyclones in the Bay of Bengal basin'. *J. Atmos. Res.*, Vol. 246, 105902, 2020 10.1016/j.atmosres.2020.105092

II. Emanuel K., : 'Increasing destructiveness of tropical cyclones over the past 30 years'. *Nature*, Vol, 436, pp. 686-688, 2005 10.1038/nature03906

III. Elsberry R. L., Jordon M. S., Vitart F., : 'Predictability of tropical cyclone events on inter seasonal time scales with the ECMWF monthly forecast model'. *Asia. Pac. J. Atmos. Sci*., Vol. 46, pp. 135-153, 2010 10.1007/s13143-010-0013-4

IV. Ghosh I., Chakravarty N., : 'Tropical cyclones: expressions for velocity components and stability parameter'. *J. Nat. Haz.*, Vol. 94, pp. 1293-1304, 2018. 10.1007/s11069-018-3477-7

V. Ghosh I., Das S., Chakravarty N., : 'A review on tropical cyclones'. *Journal of Mechanics of Continua and Mathematical Sciences*, Vol. 16(12), pp. 20-48, 2021. 10.26782/jmcms.2021.12.00003

VI. Ghosh I., Das S., Chakravarty N.,: 'RSRW Data, CSP and cyclone track prediction'. *Journal of Mechanics of Continua and Mathematical Sciences*, Vol. 17(2), pp. 41-51, 2022 10.26782/jmcms.2022.02.00005

VII. Ghosh I., Das S., Chakravarty N., : ‘Anomaly temperature in the genesis of tropical cyclone’. *J. Nat. Haz.*, Vol. 114, pp. 1477-1503, 2022. 10.1007/s11069-022-05434-4

VIII. Jung B. J., Kim H. M., Kim Y. H., Jeon E., H., Kim K. H., : ‘Observation system experiments for typhoon Jangmi (200815); observed during T-Parc’. *Asia. Pac. J. Atmos. Sci*, Vol. 46, pp. 305-316, 2010. 10.1007/s1314: 010-1007-y

IX. Köhle M. P., Promper C., Glade T., : ‘A common methodology for risk assessment and mapping of climate change related hazards- implications for climate change adaptation policies’. *MDPI Article Climate*, Vol. 4(1), 8, 2016. 10.3390/cli4010008

X. Liu L., : ‘Tropical Cyclones, Oceanic Circulation and Climate, Climate Change and Variability, Suzanne Simard (Ed.), ISBN: 978-953-307-144-2, InTech, 2010 http://www.intechopen.com/books/c change-and-variability/tropical-cyclones-oceanic-circulation-and- climate

XI. Lala S. et al., : ‘Mathematical explanation of earlier dissipation of the energy of tilted cyclone’. *J. Climatol. Weather. Forecast.*, Vol. 2(2)**,** pp. 1-6, 2014. 10.4172/2332-2594.1000115

XII. Li L., Xuyang G., : ‘Intensity change of Noru during binary tropical cyclone interaction’. *Asia. Pac. J. Atmos. Sci.*, Vol. 57, pp. 135-147, 2021. 10.1007/s13143-020-00181-7

XIII. Nott J. F., : ‘Intensity of prehistoric tropical cyclones’. *J. Geophys. Res.* Vo. 108(D7),4212, 2003. 10.1029/2002JD002726

XIV. Nelson S. A., : ‘Tropical Cyclones (Hurricanes)’. 2014. http://tulane.edu/sanelson/New_Orleans__and_Hurricanes/tropical_ cyclones.htm

XV. Posada R., Ortega G. E., Sanchez J. L., Lopez L., : ‘Verification of the MM5 model using radiosonde data from Madrid-Barajas Airport’. *J. Atmos. Res.*, Vol. 122, pp. 174-182, 2012 10.1016/j.atmosres.2012.10.

XVI. Ritchie I., Vigh J. L., : ‘Tropical cyclone structure and intensity change: Inner core impacts - Rapporteur Report, Topic 1.2’. *7th International Workshop on Tropical Cyclones* (IWTC-VII), France. 10.13140/2.1.1825.8247

XVII. Rezapour M., : ‘A new methodology of classification of tropical cyclones: the importance of rainfall’. *PhD Thesis, The University of Queensland, Australia*. 2015.

XVIII. Sikka D. R., : ‘Major advances in understanding and prediction of tropical cyclones over north Indian Ocean : A Perspective’. *Mausam* , Vol. 57(1), pp. 165-196, 2006.

XIX. Shevtsov B. M., Ekaterina P., Holzworth R. H., : ‘Relation of tropical cyclone structure with thunder storm activity’. *XXI International Symposium on Atmospheric and Ocean Optics*, Tomsk, Russian Federation. 2015. 10.1117/12.2203348

XX. Stern D. P., Vigh J. L., Nolan D., S., Zhang F., : ‘Revisiting the relationship between eyewall contraction and intensification’. *J. Atmos. Sci.*, Vol. 72(4), pp. 1283-1306, 2015. 10.1175/JAS-D-14-0261.1

XXI. Sheasarani A., Khamiki A. K., Bidhokti A. A. A., Azadi M., : ‘Sensitivity analysis of the numerical aspect of the SWAN for the tropical cyclone wave simulations in the Gulf of Oman’. *Arab. J. Geosci.*, Vol. 13, 692. 2020. 10.1007/s12517-020-05629-8

XXII. Spiridonov V., Curic M., Sladic N., Jakimovski B., : ‘Novel thunderstorms alert system (NOTHAS)’. *Asia. Pac. J. Atmos. Sci.*, Vol. 57, pp. 479-498, 2020. 10.1007/s13143-020-00210-5

XXIII. Tapiador F. J., : ‘Hurricane footprints in global climate models’. *Entropy*, Vol. 10, pp. 613-620, 2008. 10.3390/e10040613

XXIV. Zehnder J. A., : ‘Tropical cyclone’. 2020. https://www.britannica.com/science/tropical-cyclone